Diffuse Optical Multipatch Technique for Tissue Oxygenation Monitoring: Clinical Study in Intensive Care Unit

Chun-Yang Wang, Ming-Lung Chuang, Shinn-Jye Liang, Jui-che Tsai, *Member, IEEE*, Ching-Cheng Chuang, Yao-Sheng Hsieh, Chih-Wei Lu, Po-Lei Lee, and Chia-Wei Sun*

***Abstract*—Diffuse optical multipatch technique is used to assess spatial variations in absorption and scattering in biological tissue, by monitoring changes in the concentration of oxyhemoglobin and deoxyhemoglobin. In our preliminary study, the temporal tracings of tissue oxygenation are measured using diffuse optical multipatch measurement and a venous occlusion test, employing normal subjects and ICU patients suffering from sepsis and heart failure. In experiments, obvious differences in tissue oxygenation signals were observed among all three groups. This paper discusses the physiological relevance of tissue oxygenation with respect to disease.**

***Index Terms*—Diffuse optical multipatch technique, diffuse optical spectroscopic imaging (DOSI), heart failure, intensive care medicine, near-infrared spectroscopy (NIRS), oxygenation dynamics, sepsis, venous occlusion test (VOT).**

I. Introduction

In intensive care medicine, real-time physiological monitoring of vital signs plays an important role in diagnosis and therapy, particularly for the cardiovascular assessment of patients with heart failure and/or sepsis. To maintain central blood pressure and vital organ perfusion, cardiovascular insufficiency may be overcome by increasing sympathetic output through the vasoconstriction of lesser vital organs and muscles. Unfortunately, this compensatory mechanism often masks profound hypovolemia. Currently, bedside assessment of cardiovascular adequacy involves either the measurement of the vital signs, blood lactate levels, and capillary refill, or the monitoring of tissue oxygenation using invasive techniques [1]. The ability to characterize tissue oxygenation through noninvasive means would be of immense benefit in the ICU.

Over the past decade, diffuse optical spectroscopic imaging (DOSI) with near-infrared light has been shown to be an effective tool for measuring local changes in tissue oxygenation and perfusion [2], [3]. Diffuse photons (the propagation of photons through multiple scattering) penetrate through several centimeters of tissue, measuring differences in the concentrations of oxyhemoglobin (HbO_2) and deoxyhemoglobin (Hb). This technique illuminates a banana-shaped region of the penetrated tissue to a maximum depth of $d/2$ from the surface of the skin (d is the distance between the light source and the detector) [28]. Oxygenation signals are the result of light traveling through the skin and muscle, and fluctuations in the volume of blood in the tissue or changes in tissue oxygenation during vascular occlusion alter optical absorption.

Since 1986, DOSI has been utilized in the assessment of muscle perfusion [4]–[6]. To avoid having to use exogenous tracers, the analysis of abrupt changes in HbO_2 and Hb in response to vascular occlusion has been proposed [7]. This technique has demonstrated a strong correlation with xenon and plethysmographic methods, both in resting and exercising subjects [8]. In recent years, signal channel near-infrared spectroscopy (NIRS) has been applied in fields as diverse as kinematics and kidney disease; however, its low reproducibility remains problematic because oxygenation signals are influenced by the location at which the probing is performed [9], [10]. The region of the cephalic vein responds effectively to venous occlusion test (VOT); however, it cannot be located consistently in every patient [11]. This paper demonstrates that the DOSI system is capable of providing 2-D imagery of local tissue oxygenation, in which the dominant response area of concomitant oxygenation dynamics with venous occlusion may be highlighted for analysis. Because this method reduces the error associated with

Manuscript received February 10, 2011; revised April 6, 2011; accepted April 12, 2011. Date of publication April 29, 2011; date of current version December 21, 2011. This work was supported in part by the Taiwan National Science Council under Grant NSC 99-2221-E-010-011, Grant NSC 99-2622-E-010-001-CC3, Grant NSC 98-2221-E-010-004, Grant NSC 98-2221-E-002-090, and a Grant from the Ministry of Education, Aim for the Top University Plan in National Yang-Ming University, and Chang Gung Medical Research Program under Grant CMRPG32058. *Asterisk indicates corresponding author.*

C.-Y. Wang and Y.-S. Hsieh are with the Department of Photonics, National Chiao Tung University, Hsinchu 30010, Taiwan.

M.-L. Chuang is with the Divisions of Pulmonary and Department of Critical Care Medicine, Chung Shan Medical University Hospital and School of Medicine, Chung Shan Medical University, Taichung 40447, Taiwan.

S.-J. Liang is with the Divisions of Pulmonary and Critical Care Medicine, China Medical University Hospital, Taichung 40447, Taiwan.

J.-C. Tsai is with the Graduate Institute of Photonics and Optoelectronics and Department of Electrical Engineering, National Taiwan University, Taipei 10617, Taiwan.

C.-C. Chuang is with the Institute of Biomedical Engineering, National Taiwan University, Taipei 10617, Taiwan.

C.-W. Lu is with the Biomedical Technology and Device Research Labs, Industrial Technology Research Institute, Hsinchu 31040, Taiwan.

P.-L. Lee is with the Department of Electrical Engineering, National Central University, Taoyuan 32001,Taiwan.

*C.-W. Sun is with the Biophotonics Interdisciplinary Research Center and Institute of Biophotonics, National Yang-Ming University, Taipei 11221, and the Department of Photonics, National Chiao Tung University, Hsinchu 30010, Taiwan (e-mail: chiaweisun@ym.edu.tw).

Color versions of one or more of the figures in this paper are available online at http://ieeexplore.ieee.org.

Digital Object Identifier 10.1109/TBME.2011.2147315

probing location, the signal-to-noise ratio can be improved considerably.

In addition to reducing error resulting from probing location, DOSI also provides dynamic imaging, wherein changes in optical properties and/or physiological parameters are identified as they occur. The most prominent example may be the imaging of hemodynamic effects during functional or drug-induced stimulation of the brain [11], [13]. The advantage of dynamic over static imaging is that the images represent changes against a baseline defined by the system itself, and such changes are usually immune to static measurement error [14].

In our study, a diffuse optical multipatch technique with continuous wave (CW) setup was built using dual-wavelength laser diodes (LDs) as a near-infrared light source. We hypothesize that 1) noninvasive monitoring of dynamic changes in tissue oxygenation in response to venous occlusion provides an accurate representation of local metabolic rate and perfusion in local tissue; 2) this method reduces the error associated with probing in different locations; and 3) the recovery of O_2 saturation in tissue following venous occlusion characterizes preexisting cardiovascular reserves. This study provides a preliminary report on the oxygenation of muscles in the extremities measured during vessel occlusion testing in normal subjects and ICU patients suffering from sepsis and heart failure.

II. Material and Method

A. Patients

This clinical study was designed as a prospective case-controlled clinical investigation, receiving approval from the local institutional review board. Informed consent was obtained from normal volunteers but waived for patients. In the preliminary study, five patients with sepsis and seven patients with heart failure were examined in the ICU of a tertiary hospital.

Sepsis is defined as a condition characterized by whole-body inflammation due to the presence of a known or suspected infection [15]. Heart failure is the inability of the heart to supply sufficient blood flow to the human body. Patients were excluded if they had systolic blood pressure below 50 mmHg, were movable but unable to control their limbs on command, or had skin defects in the upper extremities in which the DOSI probe would be placed. Eleven healthy volunteers without cardiovascular or its related diseases, diabetes and sepsis, were treated as control subjects.

In previous studies, the thickness of adipose tissue was a factor influencing the detection of diffuse light signals [16]–[18]; however, in this study, all ICU patients appeared to underweight. The average body mass indices of patients and healthy volunteers were 20.6 and 23.6, respectively. Thus, the concomitant effect of adipose variation in DOSI measurement was disregarded.

B. Experimental Setup

DOSI depends on three critical characteristics related to the absorption spectra of tissue. First, compared to other wavelengths, near-infrared light (650–950 nm) is less susceptible to absorption by tissue, allowing it to penetrate several centimeters and still be detected. As a result, light at these wavelengths is often referred to as an "optical window" into biological tissue. The second critical characteristic of near-infrared (NIR) light is the fact that it is absorbed only by hemoglobin, myoglobin, or oxidized cytochrome; however, the contribution of the latter two to the light attenuation signal is very small. Hence, the DOSI signal is derived predominantly from hemoglobin present within the volume of tissue penetrated by NIR light. The last critical characteristic is the difference in absorption spectra between oxyhemoglobin and deoxyhemoglobin. Deoxyhemoglobin dominates the absorption below 805 nm, while oxyhemoglobin dominates above 805 nm [19], [20]. Hence, the DOSI setup included four pairs of LDs (QL78D6S and QL85D6S, QSI) as light sources at 780 and 850 nm. The optical power of LDs at both wavelengths was 1 mW, with a 5-nm bandwidth, 4 mm in diameter. The backscattered optical signals from human tissue were detected using nine photodiodes (S2387-33R, HAMAMATSU), 6 mm in diameter, arranged as four squares on a flexible probe, with the light sources placed in the center of each square. The distance of source–detector separation was 2 cm on the optode and a data acquisition card was used as a PC–optode interface, with LDs driving, multiplexing, and detected signals demultiplexing from photodiodes.

C. Venous Occlusion Test

Although inducing ischemia through arterial occlusion provides additional information on local muscular metabolic energy [21], [22], this process runs the risk of tissue necrosis in critical patients. Thus, a VOT was adopted to estimate the consumption of oxygen by muscles and blood flow using the same techniques of conventional venous plethysmography [23]. VOT was performed using a controllable pneumatic tourniquet around the upper arm, causing an increase in the volume of blood in the forearm due to undisturbed forearm arterial inflow and interrupted venous outflow. Thus, changes in HbO_2, Hb, and THb during venous occlusion were induced only through arterial inflow and the consumption of oxygen by tissue [24].

D. Protocol

In a quiet environment, subjects rested in a semirecumbent position, prohibited from moving during optical measurements of the VOT. A controllable pneumatic tourniquet provided 50 mmHg of pressure on the upper arm for venous occlusion, which was maintained for 70 s before being released. The optode of DOSI was placed on the skin of the brachioradialis muscle for the assessment of oxygenation and blood volume, through optical detection. During measurement, the optical probe was brought in close contact with the skin to prevent noise from the environmental and surface backscattering.

An initial manual blood pressure assessment was taken on the same arm to define baseline perfusion pressure using a sphygmomanometer. The sphygmomanometer was then placed on the forearm above the probe to avoid discomfort during VOT and minimize the total vascular space from which the redistribution

TABLE I
PHYSIOLOGICAL PARAMETERS OF SUBJECTS IN THE STUDY

	Normal (n=17)	Heart failure (n=13)	Sepsis (n=11)	Recuperate (n=1)	Critical (n=1)
Age (years)	27.5±3.8	74.7±11.4	50.7±8.13	44	82
MAP(mmHg)	78.7±9.8	86.8±13.3	70.8±16.9	85.3	68.3
HR (beats/min)	73.7±8.8	82.5±15.5	104.1±9.5	95	106
SpO2	97.3±1.2	98.5±1.3	91.3±12.9	99	82
Hb(g/dl)	—	10.3±1.7	9.5±2.0	9.8	9.8

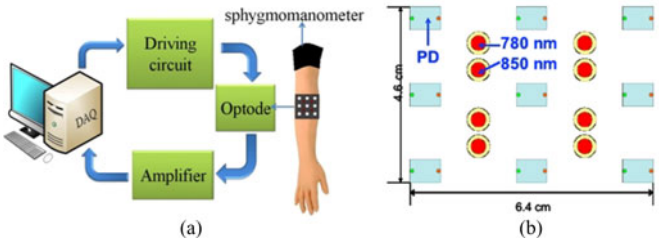

Fig. 1. (a) Schematic of DOSI system. (b) Geometrical arrangement of optode.

of blood volume might occur [25]. During the DOSI measurement, several physiological parameters such as heart rate, mean arterial pressure, oxyhemoglobin saturation were measured using pulse oximetry (SpO_2) and monitored concomitantly (see Table I).

E. Calibration

The fundamental measurement associated with the DOSI system is the intensity of light after traveling through the tissue. To ensure that the measured intensity is influenced only by the properties of the tissue, the DOSI system must be calibrated prior to measurement, by placing the optode on two different turbid materials using a known μ_a and μ_s. The intensity of the light signals was measured and analyzed according to the modified Beer–Lambert law. This enabled the extraction of experimental values of μ_a and μ_s to ensure that the degree of error between theoretical values and experimental results was less than 1%.

F. Beer–Lambert Law

All optical signals are analyzed according to the modified Beer–Lambert law with various source–detector separations on the optode (see Fig. 1). The modified Beer-Lambert law [26] is as follows:

$$\mathrm{OD} = -\log\left(\frac{I}{I_o}\right) = \varepsilon CLB + G \tag{1}$$

where OD is the optical density. I_0 and I are the intensities of incident light and detected light, respectively. ε represents the extinction coefficient of the tissue; C is the concentration of the tissue. L represents the mean path length of detected photons. B is the path length factor set for the compensation of various effective path lengths of various wavelengths. G is defined as a geometric factor used to compensate the objective with different geometrical shapes. Typically, L, B, and G are constants with monochromatic illumination in a turbid media with unchanging geometry. Changes in optical signaling were measured concomitantly with changes in the oxygenation of tissue. Then, (1) can be rewritten as

$$\Delta\mathrm{OD} = \mathrm{OD}_{\mathrm{Final}} - \mathrm{OD}_{\mathrm{Initial}} = -\log\left(\frac{I_f}{I_i}\right) = \varepsilon\Delta CLB \tag{2}$$

where ΔOD is the change in optical density. $\mathrm{OD}_{\mathrm{Final}}$ and $\mathrm{OD}_{\mathrm{Initial}}$ are the detected optical density and the optical density of incident light. I_f and I_i are the measured intensities before and after the change in concentration; ΔC is the change in concentration. Changes in detected light intensity were dominated by changes in the concentration of oxyhemoglobin and deoxyhemoglobin in the tissue. Therefore, the description can be treated as follows:

$$\Delta\mathrm{OD}^{\lambda} = \left(\varepsilon^{\lambda}_{\mathrm{HbO}_2}\cdot\Delta[\mathrm{HbO}_2] + \varepsilon^{\lambda}_{\mathrm{Hb}}\cdot\Delta[\mathrm{Hb}]\right)B^{\lambda}L \tag{3}$$

$$\Delta[\mathrm{HbO}_2] = \frac{\varepsilon^{\lambda 1}_{\mathrm{Hb}}\cdot\left(\Delta\mathrm{OD}^{\lambda 2}/B^{\lambda 2}\right) - \varepsilon^{\lambda 2}_{\mathrm{Hb}}\cdot\left(\Delta\mathrm{OD}^{\lambda 1}/B^{\lambda 1}\right)}{\varepsilon^{\lambda 1}_{\mathrm{Hb}}\cdot\varepsilon^{\lambda 2}_{\mathrm{HbO}_2} - \varepsilon^{\lambda 2}_{\mathrm{Hb}}\cdot\varepsilon^{\lambda 1}_{\mathrm{HbO}_2}} \tag{4}$$

$$\Delta[\mathrm{Hb}] = \frac{\varepsilon^{\lambda 2}_{\mathrm{HbO}_2}\cdot\left(\Delta\mathrm{OD}^{\lambda 2}/B^{\lambda 1}\right) - \varepsilon^{\lambda 1}_{\mathrm{HbO}_2}\cdot\left(\Delta\mathrm{OD}^{\lambda 1}/B^{\lambda 2}\right)}{\varepsilon^{\lambda 1}_{\mathrm{Hb}}\cdot\varepsilon^{\lambda 2}_{\mathrm{HbO}_2} - \varepsilon^{\lambda 2}_{\mathrm{Hb}}\cdot\varepsilon^{\lambda 1}_{\mathrm{HbO}_2}}. \tag{5}$$

The oxygenation saturation StO_2 and the concentration of total hemoglobin can be calculated from concentrations of oxyhemoglobin and deoxyhemoglobin based on

$$\mathrm{THb} = \mathrm{HbO}_2 + \mathrm{Hb} \tag{6}$$

$$\mathrm{StO}_2 = \frac{\mathrm{HbO}_2}{(\mathrm{HbO}_2 + \mathrm{Hb})}. \tag{7}$$

G. Analysis

In our DOSI system, all detected signals were analyzed according to the modified Beer–Lambert law for 2-D image mapping with respect to the geometry of the source–detector. The data acquisition of optical signal is achieved by using nearest neighbor source–detector measurement. The intensity of detected light can be mapped as 4×4 image via optode arrangement [as shown in Fig. 2(b)]. For detail interpretation of oxygenation distribution in tissue, the linear interpolation processing was adopted [see Fig. 2(c)]. An average of the pixel values was used to derive temporal profiles to characterize signals associated with the oxygenation of tissue. Fig. 3 presents images showing dynamic changes in oxygenation in a normal subject. The obvious response area in the image is the region of the cephalic vein. In a previous discussion, the amplitude of signals as they pertain to tissue oxygenation was related to the position from which measurements were taken. The area of weak image response did not necessarily reveal useful information with which to evaluate tissue oxygenation while monitoring VOT. To improve the signal-to-noise ratio, this study adopted a binarized segmentation method for the postprocessing of images. A threshold value [27] provided a baseline for binarized segmentation. Each image pixel could be divided into two parts: one above the threshold value and the other below. In experiments,

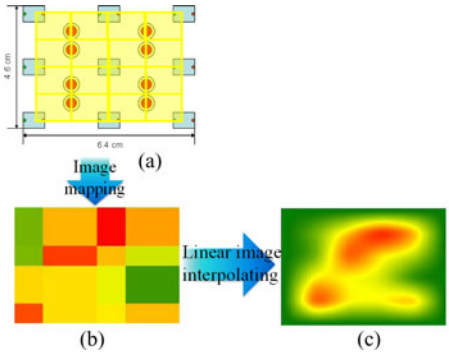

Fig. 2. Reconstructed values that are calculated with the data measured by nearest neighbor source–detector pairs. (a) Optode geometry. (b) 4 × 4 pixels image mapping. (c) Linearly interpolated imaging.

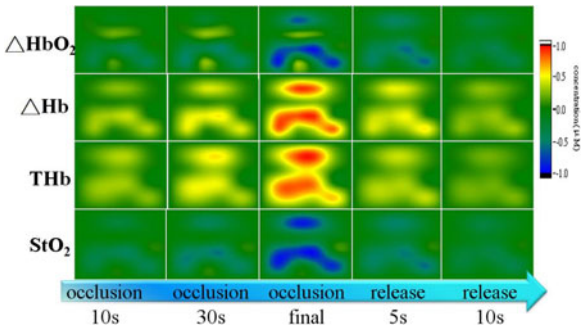

Fig. 3. Image of deoxyhemoglobin (Hb), oxyhemoglobin (HbO_2), total hemoglobin (THb), and tissue oxygen saturation (StO_2) during VOT for a normal subject.

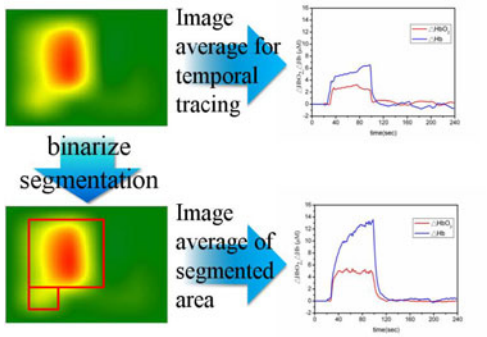

Fig. 4. Illustration of tissue oxygenation analysis with binarized segmentation from a normal subject.

the threshold value is set as average value of all pixel detected image for each subject. Fig. 4 shows the scheme used for signal processing based on a binarized segmentation method to monitor oxygenation dynamics in a DOSI system. The black area in the image represents areas without obvious detection through the tissue during VOT, due to the lower density of vessels. To observe the regional perfusion using the VOT, the average intensity of the entire DOSI image was calculated as the baseline and only the parts of the image with intensity greater than that of the baseline were then segmented. The average intensity of the segmented areas was redefined as our measured signal of tissue oxygenation. Fig. 4 shows that the VOT-induced oxygenation response improved by more than 27% following the process

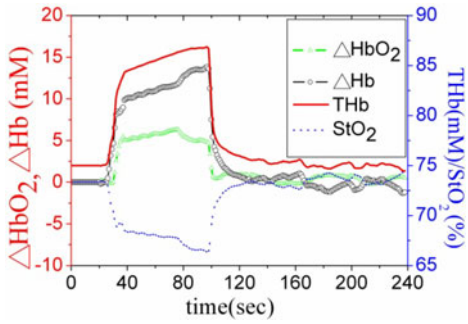

Fig. 5. Hb, HbO_2, StO_2, and THb response of a normal subject during VOT.

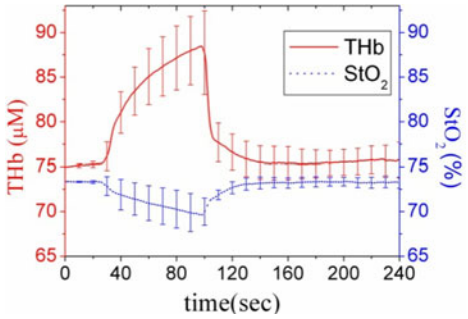

Fig. 6. Temporal tracings of a normal control tissue oxygen saturation (StO_2) and total hemoglobin (THb) response to a VOT assessment (the error bar indicates the standard deviation in the group).

of binarized segmentation. The area of dominant response of concomitant oxygenation dynamics with venous occlusion was then enhanced using binarized segmentation, because the process consumed much of the VOT correlated signal to improve the signal-to-noise ratio. This method enabled a reduction in experimental error due to probing measurement taken in different locations; that is, the oxygenation signal could be maintained even with a slight shift in the area probed. This implies that the data obtained from DOSI measurements are more useful than those derived through the detection of hemoglobin from a single source–detector pair.

III. Experimental Results

Fig. 5 shows temporal tracings of O_2 saturation in tissue (StO_2), total hemoglobin (THb), oxyhemoglobin (HbO_2), and deoxyhemoglobin (Hb), in response to a VOT of a normal representative subject. The THb signal, indicating the local volume of blood in the tissue, increased during the VOT process. The StO_2 response was covaried with changes in tissue oxygenation. Fig. 6 shows the group average response with a standard deviation of THb and StO_2 for the VOT of normal subjects.

Fig. 7 shows the THb and StO_2 curves in response to the VOT in patients with heart failure. Obviously, the average response of THb for patients with heart failure is lower and more slurred than that of normal subjects. A stepwise decreasing pattern in patients with heart failure characterized StO_2 tracing.

Tracings of oxygenation in tissue during the VOT of patients with sepsis are shown in Fig. 8. The curves show a slight, slow increase in the THb tracing and a decrease in StO_2 tracing.

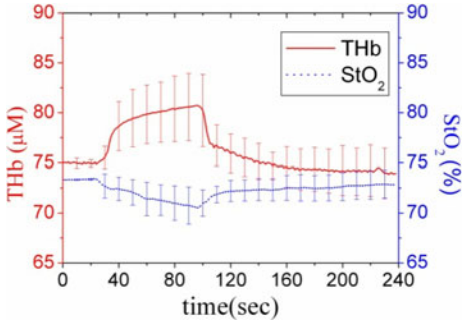

Fig. 7. Temporal tracings of the VOT response from heart failure patients (the error bar indicates the standard deviation in the group).

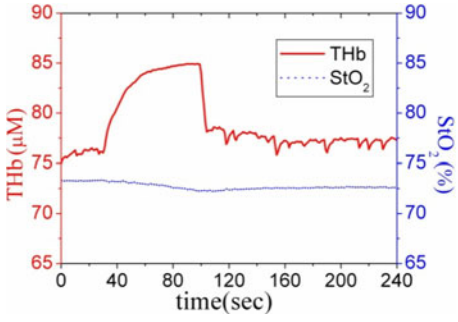

Fig. 10. Temporal tracings of the VOT response from a recuperative patient of sepsis.

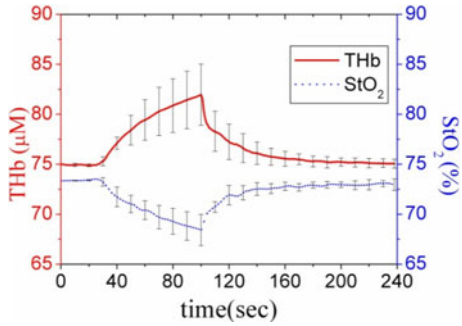

Fig. 8. Temporal tracings of the VOT response from septic patients (the error bar indicates the standard deviation in the group).

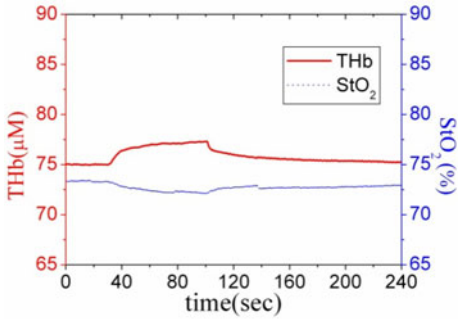

Fig. 11. Temporal tracings of the VOT response from a critical sepsis patient.

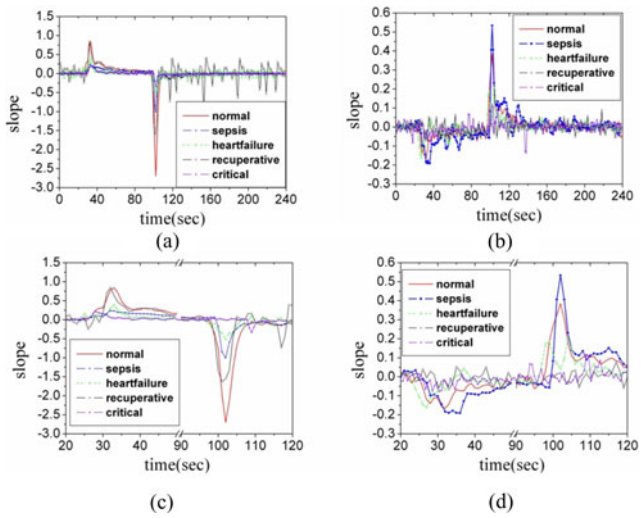

Fig. 9. Temporal differentials of (a) THb and (b) StO_2 from various subjects. Zoom in curves from (c) occlusion (30 s) to (d) release (100 s).

Fig. 9(a) and (b) shows temporal differentials of THb/StO_2 from all subjects in the VOT experiments including 17 normal subjects, 13 patients with heart failure, 11 patients with sepsis, a recuperative patient with sepsis, and a critical patient with serious sepsis. Fig. 9(c) and (d) shows the zoomed in curves from occlusion (30 s) to release (100 s). The lower rate of change in the oxygenation of patients with heart failure or sepsis than that of the controlled group indicates an insufficient supply of oxygen to the extremities. Although we had only one recuperative patient with sepsis, the increases in THb and StO_2 were higher than those of patients with sepsis (see Fig. 10). Fig. 11 shows the oxygenation dynamics from VOT for a patient in critical condition. The weak response of THb and StO_2 indicate that the patient was in extremis. Based on the major two characteristics: 1) the responded intensity of oxygenation change during VOT and 2) the temporal differentials of oxygenation dynamics at occlusion and release period (as shown in Fig. 9), the experimental results imply that the pattern of oxygenation might be used as a helpful tool for clinical diagnosis.

IV. Discussions

Generally, temporally applied low cuff pressures (50 mmHg in our cases) occlude venous outflow while minimizing the obstruction of arterial inflow [28]. An increase in deoxygenated blood is then used to determine the level of oxygenation in muscle [29]. NIRS assesses the level of oxygenation and the volume of blood in local tissue, and VOT has been shown to provide results in agreement with those obtained from traditional measurements employing plethysmography with calculations based on the Fick principle [30]. Traditional measures are unable to provide local detection within muscle tissue; however, the DOSI is capable of accessing the spatial distribution of tissue oxygenation, and to do so in real time [31].

The experimental data of the healthy subjects are consistent with previous studies [32]. StO_2 is strongly correlated with central venous saturation [33], implying that patients suffering from heart failure exhibit a lower degree of deoxygenation or oxygenation compared with the controls, due to the failure of the heart to pump resulting in musculoskeletal hypoperfusion [34].

Sepsis is considered a microcirculation disease that induces microvascular dysfunction. Due to decreases in microcircula-

tory vascular density resulting from derangement caused by sepsis [22], [32], the signal associated with the oxygenation of tissue changes slowly, implying that the vessels are intermittently perfused. Thus, these experimental results imply a faulty autoregulation of local blood flow. In Fig. 10, the results indicate a recovery of microcirculation, suggesting the feasibility of clinical diagnosis based on DOSI measurements. For qualitative comparisons, the greatest change in tissue oxygenation occurred at the beginning of VOT in healthy subjects, particularly with regard to changes in the concentration of oxyhemoglobin. Moreover, changes in the curves related to the concentration deoxyhemoglobin differed considerably among the three groups. As previously mentioned, different temporal tracings revealed different physiological conditions. Nevertheless, the recovery time of total hemoglobin was longer in septic patients than in others. Although the number of subjects in this study was small, the measurement of tissue oxygenation during VOT based on DOSI revealed the possibility of wide ranging clinical applications.

In conclusion, we determined the following. 1) Different temporal tracings reveal different physiological conditions. We were able to build a database of several physiological conditions and speculate that this technique could render an index capable of providing assistance in clinical diagnosis. Such an approach would be highly valuable for examining the effects of medication in the ICU. 2) The application of the binarized segmentation method from a 2-D image could reduce error due to artifacts resulting from probing in different locations, thereby increasing the accuracy of DOSI. 3) The diffuse optical multipatch system comprises commercially available electronic components such as LDs and photodiodes, thereby minimizing instrumentation and costs [35]. Thus, the system could be used as a homecare device in the same manner as sphygmomanometers or blood sugar monitors.

REFERENCES

[1] Y. Hoshi, "Functional near-infrared spectroscopy: Current status and future prospects," *J. Biomed. Opt.*, vol. 12, p. 062106, 2007.

[2] C. Zhou, S. A. Eucker, T. Durduran, G. Yu, J. Ralston, and S. H. Friess, "Diffuse optical monitoring of hemodynamic changes in piglet brain with closed head injury," *J. Biomed. Opt.*, vol. 14, no. 3, p. 034015, 2009.

[3] S. P. Nighseander-Rempel, V. V. Kupriyanov, and R. A. Shaw, "Regional cardiac tissue oxygenation as a function of blood flow and pO_2: A near-infrared spectroscopic imaging study," *J. Biomed. Opt.*, vol. 11, no. 5, p. 054004, 2006.

[4] R. Wariar, J. N. Gaffke, R. G. Haller, and L. A. Bertocci, "A modular NIRS system for clinical measurement of impaired skeletal muscle oxygenation," *J. Appl. Physiol.*, vol. 88, pp. 315–325, 2000.

[5] A. Yodh and B. Chance, "Spectroscopy and imaging with diffusing light," *Phys. Today*, vol. 48, pp. 34–40, 1995.

[6] Y. Lin, G. Lech, S. Nioka, X. Intes, and B. Chance, "Noninvasive, low-noise, fast imaging of blood volume and deoxygenation changes in muscles using light-emitting diode continuous-wave imager," *Rev. Sci. Instrum.*, vol. 73, no. 8, p. 3065, 2002.

[7] C. Casavola, L. A. Paunescu, S. Fantini, and E. Gratton, "Blood flow and oxygen consumption with near-infrared spectroscopy and venous occlusion: spatial maps and the effect of time and pressure of inflation," *J. Biomed. Opt.*, vol. 5, no. 3, pp. 269–276, 2000.

[8] R. A. De Blasi, M. Ferrari, A. Natali, G. Conti, A. Mega, and A. Gasparetto, "Noninvasive measurement of forearm blood flow and oxygen consumption by near-infrared spectroscopy," *J. Appl. Physiol.*, vol. 76, pp. 1388–1393, 1994.

[9] T. Hamaoka, K. K. McCully, V. Quaresima, K. Yamamoto, and B. Chance, "Near-infrared Spectroscope/imaging for monitoring muscle oxygenation and oxidative metabolism in healthy and diseased humans," *J. Biomed. Opt.*, vol. 12, no. 6, p. 062105, 2007.

[10] M. K. Erb, D. K. Chen, A. Sassaroli, S. Fantini, and P. R. Bergaethon, "Diffuse optical signals in response to peripheral nerve stimulation reflect skeletal muscle kinematics," *Biomed. Opt. Exp.*, vol. 1, no. 3, p. 943, 2010.

[11] J. Sobotta, *Sobotta Atlas of Human Anatomy*. Munich, Germany: Urban & Schwarzenberg, 1990.

[12] V. Toronov, A. Webb, J. H. Choi, M. Wolf, L. Safonova, U. Wolf, and E. Gratton, "Study of local cerebral hemodynamics by frequency-domain near-infrared spectroscopy and correlation with simultaneously acquired functional magnetic resonance imaging," *Opt. Exp.*, vol. 9, no. 8, pp. 417–427, 2001.

[13] S. G. Diamond, T. J. Huppert, V. Kolehmainen, M. A. Franceschini, J. P. Kaipio, S. R. Arridge, and D. A. Boas, "Dynamic physiological modeling for functional diffuse optical tomography," *Neuroimage*, vol. 30, pp. 88–101, 2006.

[14] J. M. Lasker, J. M. Masciotti, M. Schoenecker, C. H. Schmitz, and A. H. Hielscher, "Digital-signal-processor-based dynamic imaging system for optical tomography," *Rev. Sci. Instrum.*, vol. 78, p. 083706, 2007.

[15] R. C. Bone, R. A. Balk, and F. B. Cerra, "Definitions for sepsis and organ failure and guidelines for the use of innovative therapies in sepsis,," *Chest*, vol. 101, pp. 1644–1655, 1992.

[16] M. C. P. VanBeekvelt, M. S. Borghuis, B. G. M. Van Engelen, R. A. Wevers, and W. N. J. M. Colier, "Adipose tissue thickness affects *in vivo* quantitative near-IR spectroscopy in human skeletal muscle," *Clin. Sci.*, vol. 101, pp. 21–28, 2001.

[17] H. Gómez, J. Mesquida, P. Simon, H. K. Kim, J. C Puyana, C. Ince, and M. R Pinsky, "Characterization of tissue oxygen saturation and the vascular occlusion test: Influence of measurement mites, probe size and deflation," *Critical Care*, vol. 13, suppl. 5, p. S3, 2009.

[18] R. Bezemer, A. Lima, D. Myers, E. Klijn, M. Heger, P. T. Goedhart, J. Bakker, and C. Ince, "Assessment of tissue oxygen saturation during a vascular occlusion test using near-infrared spectroscopy: The role of probe spacing and measurement site studied in healthy volunteers," *Critical Care*, vol. 13, suppl. 5, p. S4, 2009.

[19] G. Strangman, D. A. Boas, and J. P. Sutton, "Noninvasive neuroimaging using near-infrared light," *Biol. Psychiatry*, vol. 52, pp. 679–693, 2002.

[20] R. Cubeddu, A. Pifferi, P. Taroni, A. Torricelli, and G. Valentini, "Noninvasive absorption and scattering spectroscopy of bulk diffusive media: An application to the optical characterization of human breast," *Appl. Phys. Lett.*, vol. 74, pp. 874–876, 1999.

[21] R. A. Meyer, "A linear model of muscle respiration explains monoexponential phosphocreatine changes," *Am. J. Physiol.*, vol. 254, pp. C548–C553, 1988.

[22] R. A. De Blasi, S. Palmicani, D. Alampi, M. Mercieri, R. Romano, S. Collini, and G. Pinto, "Microvascular dysfunction and skeletal muscle oxygenation assessed by phase-modulation near-infrared spectroscopy in patients with septic shock," *Intensive Care Med.*, vol. 31, pp. 1661–1668, 2005.

[23] M. Girardis, L. Rinaldi, S. Busani, I. Flore, S. Mauro, and A. Pasetto, "Muscle perfusion and oxygen consumption by near-infrared spectroscopy in septic-shock and non-septic-shock patients," *Intensive Care Med.*, vol. 29, pp. 1173–1176, 2003.

[24] G. Pinchler, K. Grossauer, E. Peichl, A. Gaster, A. Berghold, G. Schwantzer, H. Zotter, W. Muller, and B. Urlesberger, "Combination of different noninvasive measuring techniques: A new approach to increase accuracy of peripheral near infrared spectroscopy," *J. Biomed. Opt*, vol. 14, no. 1, p. 014014, 2009.

[25] H. Gómez, A. Torres, P. Polanco, H. K. Kim, S. Zenker, J. C. Puyana, and M. R. Pinsky, "Use of noninvasive NIRS during a vascular occlusion test to assess dynamic tissue O_2 saturation response," *Intensive Care Med.*, vol. 34, pp. 1600–1607, 2008.

[26] D. A. Boas, T. Gaudette, G. Strangman, X. Cheng, J. J. A. Marota, and J. B. Mandeville, "The accuracy of near infrared spectroscopy and imaging during focal changes in cerebral hemodynamics," *NeuroImage*, vol. 13, pp. 76–90, 2001.

[27] M. Petrou and P. Bosdogianni, *Image Processing the Fundamentals*. New York: Wiley, 1999.

[28] G. Pichler, M. Wolf, C. Rollc, M. A. Weindling, G. Greisen, S. P. Wardle, P. Zaeamella, G. Naulaers, A. Pellicer, T. Austin, M. Bartocci, and B. Urlesberger, "Recommendations to increase the validity and comparability of peripheral measurements by near infrared spectroscopy in neonates," *Neonatology*, vol. 94, pp. 320–322, 2008.

[29] T. Hamaoka, K. K. McCully, V. Quaresima, K. Yamamoto, and B. Chance, "Near-infrared spectroscope/imaging for monitoring muscle oxygenation and oxidative metabolism in healthy and diseased humans," *J. Biomed. Opt*., vol. 12, no. 6, p. 062105, 2007.
[30] M. C. P. Van Beekvelt, W. N. J. M. Colier, R. A. Wevers, and B. G. M. Van Engelen, "Performance of near-infrared spectroscopy in measuring local O_2 consumption and blood flow in skeletal muscle," *J. Appl. Physiol*., vol. 90, pp. 511–519, 2001.
[31] S. R. Arridge, "Optical tomography in medical imaging," *Inverse Problems*, vol. 15, pp. R41–R93, 1999.
[32] J. Creteur, T. Carollo, G. Soldati, G. Buchele, D. De Backer, and J. L. Vincent, "The prognostic value of muscle StO2 in septic patients," *Intensive Care Med*., vol. 33, pp. 1549–1556, 2007.
[33] J. Mesquida, J. Masip, G. Gili, A. Artigas, and F. Baigorri, "Thenar oxygen saturation measured by near infrared spectroscopy as a noninvasive predictor of low central venous oxygen saturation in septic patients," *Intensive Care Med*, vol. 35, pp. 1106–1109, 2009.
[34] Z. Chati, F. Zannad, B. Robin-Lherbier, J. M. Escanye, C. Jeandel, J. Robert, and E. Aliot, "Contribution of specific skeletal muscle metabolic abnormalities to limitation of exercise capacity in patients with chronic heart failure: A phosphorus 31 nuclear magnetic resonance study," *Amer. Heart J*., vol. 128, pp. 781–792, 1994.
[35] S. M. Aziz, F. Khambatta, T. Vaithianathan, J. C. Thomas, J. M. Clark, and R. Marshall, "A near infrared instrument to monitor relative hemoglobin concentrations of human bone tissue in vitro and in vivo," *Rev. Sci. Instrum*., vol. 81, p. 043111, 2010.

Chun-Yang Wang received the B.S. degree in physics from Fu Jen Catholic University, Xinzhuang, Taiwan, in July 2008. He is currently working toward the M.S. degree in Display Institute, National Chiao Tung University, Hsinchu, Taiwan.

His research interest includes biophotonics.

Ming-Lung Chuang was born in Taiwan, in 1959. He received the M.D. degree from China Medical University, Taichung, Taiwan, in 1985

From 1992 to 2004, he was an Attending Physician at the Department of Chest Medicine, Chang Gung Memorial Hospital. From 1997 to 1999, he, as a Visiting Scientist, followed Prof. K. Wasserman of Harbor-UCLA Medical Center, Torrance, CA, to research on exercise physiology and the clinical application of NIRS. He is currently an Associate Professor at the School of Medicine, Chung Shan Medical University, Taichung, Taiwan, and the Chief of the Department of Critical Care Medicine, Chung Shan Medical University Hospital, Taichung. He has been contributed to more than 30 peer-review journal papers. His current research interests include exercise physiology, critical care medicine, and NIRS in clinical applications

Shinn-Jye Liang was born in Taiwan, in 1971. He received the B.S. and M.S. degrees from the China medical University, Taichung, Taiwan.

Since 2006, he has been at the Division of Pulmonary and Critical Care, Department of Internal Medicine, China Medical University Hospital where he is currently an Attending Physician. His research interests include general pulmonary medicine, critical care, and sleep medicine.

Jui-che Tsai (M'09) received the B.S. degree in electrical engineering from National Taiwan University (NTU), Taipei, Taiwan, in 1997, the M.S. degree in electro-optical engineering from the Graduate Institute of Electro-Optical Engineering (currently GIPO) at NTU, in 1999, and the Ph.D. degree in electrical engineering from the University of California, Los Angeles, in 2005.

Between 1999 and 2001, he served in the military as a Second Lieutenant. Before joining the faculty of NTU, he was a Postdoctoral Researcher in the Department of Electrical Engineering and Computer Sciences and Berkeley Sensor and Actuator Center, University of California, Berkeley. He is currently an Associate Professor at the Graduate Institute of Photonics and Optoelectronics and the Department of Electrical Engineering, NTU. His research interests include optical microelectromechanical systems (MEMS), MEMS technologies, optical fiber communication, and biophotonics.

Ching-Cheng Chuang received the B.S. and M.S. degrees in biomedical engineering from Chung Yuan Christian University, Chung Li, Taiwan, in July 2003 and July 2005, respectively. He is currently working toward the Ph.D. degree at the Institute of Biomedical Engineering, National Taiwan University, Taipei, Taiwan.

His research interests include biophotonics, bio-optical signal/image processing, and optical device design.

Yao-Sheng Hsieh received the B.S. and M.S. degrees from the National Taiwan University of Science and Technology, Taipei, Taiwan. He is currently toward the Ph.D. degree at National Chiao Tung University, Hsinchu, Taiwan.

His research interests include the optical imaging methods, clinical applications, and novel optical diagnosis tool for dentistry.

Chih-Wei Lu received the Ph.D. degree in photonics and optoelectronics from National Taiwan University, Taipei, Taiwan, in January 2008.

In February 2008, he joined the Medical Electronics and Device Technology Center, Industrial Technology Research Institute, Hsinchu, Taiwan, where he is involved in developing commercial biophotonics imaging systems. He has quite a lot of experience in various OCT systems, solid-state laser, and fiber optics. He has published more than 50 prestigious journals and international conference papers. His current research interests include the application of colorectal cancer diagnosis based on optical imaging systems.

Po-Lei Lee was born in 1973. He received the B.S. degree in electrical engineering from National Cheng-Kung University, Tainan, Taiwan, in 1995, and the Ph.D. degree from the Institute of Biomedical Engineering, National Yang-Ming University, Taipei, Taiwan, in 2000.

From 2001 to 2005, he was a Postdoctoral Fellow at the Taipei Veterans General Hospital, researching the signal and image analysis procedures for electroencephalography (EEG) and magnetoencephalography (MEG) signals. He joined the Department of Electrical Engineering, National Central University, Taoyuan, Taiwan, in 2005. His research interests include signal and image processing of EEG and MEG signals as well as designing the EEG-based brain–computer interfaces.

Chia-Wei Sun was born in Taiwan in 1975. He received the B.Sc. degree in electrical engineering from National Cheng-Kung University, Tainan, Taiwan, in 1997, the M.Sc. degree in biomedical engineering from National Yang-Ming University, Taipei, Taiwan, in 1999, and the Ph.D. degree from the Institute of Photonics and Optoelectronics from National Taiwan University, Taipei, in 2003.

From 2003 to 2008, he was at the Medical Electronics and Device Technology Center, Industrial Technology Research Institute, and involved in clinical applications of biomedical optical imaging. In Summer 2005, he joined the Computational Optics Group at the University of Tsukuba, Ibaraki, Japan, as a Visiting Professor. He is currently an Assistant Research Fellow at the Biophotonics Interdisciplinary Research Center, National Yang-Ming University, and a Concurrent Assistant Professor at the Department of Photonics, National Chiao Tung University, Hsingchu, Taiwan. He has contributed to more than 40 peer-reviewed journal papers. His current research interests include diffuse optical tomography, near-infrared spectroscopy, optical coherence tomography, optics in brain science, and clinical applications based on biomedical optical imaging techniques.